Muscle wasting in patients with end-stage renal disease or early-stage lung cancer: common mechanisms at work

Julien Aniort[1,2], Alexandre Stella[3], Carole Philipponnet[1,2], Anais Poyet[1,4], Cécile Polge[1], Agnès Claustre[1], Lydie Combaret[1], Daniel Béchet[1], Didier Attaix[1], Stéphane Boisgard[5], Marc Filaire[6], Eugénio Rosset[7], Odile Burlet-Schiltz[3], Anne-Elisabeth Heng[1,2] & Daniel Taillandier[1]* 🆔

[1]INRA, Université Clermont Auvergne, UMR 1019, Human Nutrition Unit (UNH), CNRH Auvergne (Centre de Recherche en Nutrition Humaine d'Auvergne), Clermont-Ferrand, France, [2]Nephrology, Dialysis and Transplantation Department, Gabriel Montpied University Hospital, University Hospital of Clermont-Ferrand, Clermont-Ferrand, France, [3]Institut de Pharmacologie et de Biologie Structurale, Université de Toulouse, Centre National de la Recherche Scientifique, Université Paul Sabatier, France, [4]Nephrology Department, Hospital of Roanne, Roanne, France, [5]Orthopedic Surgery Department, Gabriel Montpied University Hospital, University Hospital of Clermont-Ferrand, Clermont-Ferrand, France, [6]Thoracic Surgery Department, Gabriel Montpied University Hospital, University Hospital of Clermont-Ferrand, Clermont-Ferrand, France, [7]Vascular Surgery Department, Gabriel Montpied University Hospital, University Hospital of Clermont-Ferrand, Clermont-Ferrand, France

Abstract

Background Loss of muscle mass worsens many diseases such as cancer and renal failure, contributes to the frailty syndrome, and is associated with an increased risk of death. Studies conducted on animal models have revealed the preponderant role of muscle proteolysis and in particular the activation of the ubiquitin proteasome system (UPS). Studies conducted in humans remain scarce, especially within renal deficiency. Whether a shared atrophying programme exists independently of the nature of the disease remains to be established. The aim of this work was to identify common modifications at the transcriptomic level or the proteomic level in atrophying skeletal muscles from cancer and renal failure patients.
Methods Muscle biopsies were performed during scheduled interventions in early-stage (no treatment and no detectable muscle loss) lung cancer (LC), chronic haemodialysis (HD), or healthy (CT) patients ($n = 7$ per group; 86% male; 69.6 ± 11.4, 67.9 ± 8.6, and 70.2 ± 7.9 years $P > 0.9$ for the CT, LC, and HD groups, respectively). Gene expression of members of the UPS, autophagy, and apoptotic systems was measured by quantitative real-time PCR. A global analysis of the soluble muscle proteome was conducted by shotgun proteomics for investigating the processes altered.
Results We found an increased expression of several UPS and autophagy-related enzymes in both LC and HD patients. The E3 ligases MuRF1 (+56 to 78%, $P < 0.01$), MAFbx (+68 to 84%, $P = 0.02$), Hdm2 (+37 to 59%, $P = 0.02$), and MUSA1/Fbxo30 (+47 to 106%, $P = 0.01$) and the autophagy-related genes CTPL (+33 to 47%, $P = 0.03$) and SQSTM1 (+47 to 137%, $P < 0.01$) were overexpressed. Mass spectrometry identified >1700 proteins, and principal component analysis revealed three differential proteomes that matched to the three groups of patients. Orthogonal partial least square discriminant analysis created a model, which distinguished the muscles of diseased patients (LC or HD) from those of CT subjects. Proteins that most contributed to the model were selected. Functional analysis revealed up to 238 proteins belonging to nine metabolic processes (inflammatory response, proteolysis, cytoskeleton organization, glucose metabolism, muscle contraction, oxidant detoxification, energy metabolism, fatty acid metabolism, and extracellular matrix) involved in and/or altered by the atrophying programme in both LC and HD patients. This was confirmed by a co-expression network analysis.
Conclusions We were able to identify highly similar modifications of several metabolic pathways in patients exhibiting diseases with different aetiologies (early-stage LC vs. long-term renal failure). This strongly suggests that a common atrophying programme exists independently of the disease in human.

Keywords Proteomics; Skeletal muscle; Proteasome; Autophagy; Renal failure; Cancer

Introduction

Loss of muscle mass worsens many diseases (e.g. diabetes, cancer, heart failure, respiratory failure, renal failure, and sepsis), which is known as cachexia.[1] Cachexia contributes to the frailty syndrome and is associated with impaired quality of life and increased risk of death whatever the causal disease.[2]

Cachexia is the consequence of profound changes in the metabolism of skeletal muscle fibres.[3–5] The decrease in muscle mass is due to an imbalance in protein synthesis and proteolysis in favour of the latter. Activation of proteolysis appeared to play a major role in the occurrence of muscle atrophy for rapid degradation of myofibrillar proteins in numerous catabolic models. The ubiquitin proteasome system (UPS) and autophagy are the predominant proteolytic systems involved.[6–10] The UPS is crucial for the atrophying process as it controls both the degradation of contractile proteins and the repression of protein synthesis.[8,9] The UPS targets the proteins to be degraded by linking covalently a ubiquitin (Ub) chain to the substrates to be degraded, which enables the 26S proteasome to recognize and degrade the targets.[11] The Ub chain is catalysed, thanks to an enzymatic cascade (E1, E2, and E3), with E3s that recognize the substrates and E2s that generally bring the catalytic activity. In rodent atrophying muscles, several genes (Ub, 26S proteasome subunits, E2s, E3s, etc.) are up-regulated in most catabolic situations including two muscle-specific E3 ligases, muscle atrophy F-box (MAFbx or atrogin1) and muscle ring finger-1 (MuRF1). Although data are scarce in humans, MAFbx and MuRF1 up-regulation was observed in some catabolic conditions.[6]

The mechanisms involved in the control of muscle mass during cachexia can be grouped into three categories: nutrition imbalance, mechanical stress, and neuro-hormonal mediators. Indeed, a spontaneous reduction of food intake[12,13] and a reduction in physical activity[14,15] are frequently encountered in many cases of cachexia, and starvation or muscle inactivity is sufficient to induce muscle proteolysis and atrophy.[16,17] However, this only partly explains muscle loss as increased food intake or physical activity is insufficient to prevent the occurrence of cachexia in the absence of the treatment of the causal pathology.[18] Several experiments have shed light on the role of hormonal mediator in different rodent models of cachexia. Indeed, increased levels of proinflammatory cytokines (interleukin-1 and interleukin-6 or tumour necrosis factor alpha),[19–21] resistance to insulin-like growth factor-1 and insulin,[22,23] or increased myostatin levels[24,25] were often observed. Studies on the mechanisms of muscle wasting conducted in humans remain rare,

especially during failure, but some abnormalities described in animal models have been confirmed. For example, increased levels of myostatin have been found in the *rectus abdominis muscles* of patients with chronic renal failure.[26] However, it still remains to establish whether the modifications observed are directly linked to the atrophying programme or whether they are specific of the disease itself. In addition, animal models mostly use young growing rodents, and muscle wasting is generally studied within 1–2 weeks after catabolic stimuli. This is very different from human diseases where it is generally detected within longer periods and in adults. Moreover, the physiology of rodents is not strictly comparable with that of humans. Proteomic studies coupled with bioinformatics analysis make it possible to detect proteins that potentially interact and are involved in a common biological process during muscle cachexia. Yet few have been conducted in human.[27]

It is thus crucial to identify (i) the cellular processes modified in human atrophying skeletal muscles and (ii) whether common proteome modifications characterize muscle atrophy independently of the disease in both early and late stages. In this study, we used muscles from early-stage lung cancer (LC) or late-stage chronic haemodialysis (HD) patients for investigating the role of proteolytic systems and for identifying the metabolic processes modified either at the transcriptomic level or at the proteomic level.

Material and methods

Population

This study was performed at the University Hospital of Clermont-Ferrand (France) on muscle biopsies from three groups of patients: early-stage LC, chronic HD, and healthy (CT) volunteers. Patients included were over 18 years old, with either newly diagnosed LC (for whom surgical resection was programmed by thoracotomy) or end-stage renal failure treated for at least 6 months by HD and necessitating femoral bypass revascularization. The control group patients required hip replacement for osteoarthritis. An activation of caspase-3 was noticed in such patients.[28] However, Workeneh *et al.* performed the biopsies after 1–1.5 h of surgery. As surgery increases C-reactive protein (CRP), interleukin-6, and protein degradation per se (overexpression of MuRF1 and MAFbx),[29,30] caspase-3 activity might have been elevated because of sampling delay. We therefore took the biopsies right after skin incision and verified that CT patients exhibited normal CRP level (median value 3 mg/L).

Exclusion criteria were acute or chronic infections, diabetes mellitus, corticosteroid or hormone therapy, or pregnancy. Glomerular filtration rate of LC and CT patients was estimated by the Chronic Kidney Disease Epidemiology Collaboration equation and had to be >90 mL/min/1.73 m². Patients in the HD and CT groups did not exhibit active neoplasia for at least 1 year after muscle biopsy. A CRP > 10 mg, which was measured in serum using an automated hospital-based technique (Abbott TDX), was an exclusion criterion for CT patients. All patients gave written informed consent prior to study entry. The study (DGS-2008-A00479-46) was approved by the Sud Est VI Research Ethics Committee and was conform to the standards set by the Declaration of Helsinki.

Muscles biopsies

Surgical muscle biopsies were taken at the beginning of the intervention, using a cold scalpel, in the *latissimus dorsi* (LC group) or the *vastus lateralis* (HD and CT groups). Biopsies were immediately frozen in liquid nitrogen and stored at −80°C.

Quantitative real-time PCR

Using a small fraction (≈100 mg) of the biopsies, total RNA was extracted as described by Chomczynski and Sacchi.[31] mRNA levels of E3 ligases (MuRF1, MAFbx, Nedd4, Fbxo30/MUSA1, Trim32, Hdm2, Ozz, and E4B), E2 Ub-conjugating enzymes (UBE2A, UBE2B, UBE2D, UBE2E1, UBE2G1, UBE2J1, UBE2J2, UBE2L3, UBE2V1, UBE2V2, and UBE2N), proteasome subunits (PSMA1, PSMA3, PSMB1, PSMC1, PSMD2, PSMD4, PSMD7, and PSMD13), markers of apoptosis (Csp3, Csp9, Bax, and Bcl2), autophagy (CTPL and SQSTM1), and ATF4 pathway (4EBP1, ATF4, and CHOP) were determined by quantitative real-time PCR (qRT-PCR). Reverse transcription of total RNA was performed using the QuantiTect® Reverse Transcription kit (Qiagen®). qPCR was performed using the FastStart DNA Master SYBR Green I kit (Roche), according to the manufacturer's instructions using a CFX96 thermocycler (Bio-Rad, Hercules, CA, USA). Calculations were made using the comparative ΔCt method with YWHAZ, HPRT1, and 36B4 housekeeping genes. List of primers used is provided in Supporting Information, *Table S1*.

Protein extraction

A portion (≈400 mg) of the muscle biopsies was homogenized using a Polytron® (Kinematica, Littau-Luzern, Switzerland) in 8 mL of lysis buffer [50 mM 3-(N-morpholino)propanesulfonic acid pH 7.5, 5 mM ethylenediaminetetraacetic acid pH 8.0, 1 mM phenylmethanesulfonyl fluoride, protease inhibitor cocktail (10 μL/mL of lysis buffer) (Sigma, St Louis, MO, USA), N-ethylmaleimide 10 mM, and Triton X100 1%]. Muscle homogenates were centrifuged at 16 000 *g* (4°C, 10 min), and the supernatant containing the cytoplasmic fraction was aliquoted and frozen at −80°C until use. Protein concentration was measured by absorption spectrophotometry (OD 562 nm) using the BCA kit (Pierce, Rockford, IL, USA) with bovine serum albumin as a standard.

Sodium dodecyl sulfate–polyacrylamide gel electrophoresis loading and nano-liquid chromatography–tandem mass spectrometry analysis of proteins

After reduction and alkylation, 50 μg of proteins were loaded on a 12% acrylamide sodium dodecyl sulfate–polyacrylamide gel electrophoresis gel. Proteins were visualized by Coomassie Blue staining. Each band was cut into a single slice that was washed in 100 mM ammonium bicarbonate for 15 min, followed by a second wash in 100 mM ammonium bicarbonate:acetonitrile (1:1) for 15 min. Both washes were performed at 37°C. Second cycle of washes in ammonium bicarbonate and ammonium bicarbonate/acetonitrile was then performed. Proteins were digested by incubating each gel slice with 1 μg of modified sequencing grade trypsin in 50 mM ammonium bicarbonate overnight at 37°C. The resulting peptides were extracted from the gel in three steps: a first incubation in 50 mM ammonium bicarbonate for 15 min at 37°C and two incubations in 10% formic acid:acetonitrile (1:1) for 15 min at 37°C. The three collected extracts were pooled with the initial digestion supernatant, dried in a SpeedVac, and resuspended with 50 μL of 5% acetonitrile and 0.05% trifluoroacetic acid. The peptides were analysed by nano-liquid chromatography–tandem mass spectrometry (MS/MS) using an UltiMate 3000 RSLCnano system (Dionex, Amsterdam, The Netherlands) coupled to an OrbiTrap Fusion mass spectrometer (Thermo Scientific, Bremen, Germany). Five microliters of each sample was loaded onto a C18 pre-column (300 μm id, 5 mm; Dionex), at 20 μL/min, in 5% acetonitrile and 0.05 W% trifluoroacetic acid. After 5 min of desalting, the pre-column was switched on line with the analytical C18 column (75 μm id × 15 cm C18 column; packed in-house with ReproSil-Pur C18-AQ 3 μm resin, Dr Maisch; Proxeon Biosystems), equilibrated in 95% solvent A (5% acetonitrile and 0.2% formic acid) and 5% solvent B (80% acetonitrile and 0.2% formic acid). Peptides were eluted using a 5–50% gradient of solvent B over 130 min and at a flow rate of 300 nL/min.

The OrbiTrap Fusion was operated in Data Dependent Acquisition mode to automatically switch between full scan MS and MS/MS acquisition using Xcalibur software. Survey scan MS was acquired in the Orbitrap over the m/z 300–2000 range, with the resolution set to a value of 120 000

(m/z 400). The most intense ions per survey scan were selected for higher-energy collisional dissociation fragmentation (time between Master scans: 3 s), and the resulting fragments were analysed in the linear ion trap. Dynamic exclusion was employed within 60 s to prevent repetitive selection of the same peptide.

Bioinformatics analysis of mass spectrometry raw files

Mass spectrometry raw files were analysed using the Proline software version 1.6. MS/MS spectra were searched in the Mascot search engine against the forward and reverse Human SwissProt database combined with a commonly observed contaminants list. The digestion enzyme was set to trypsin/with up to two missed cleavages. Methionine oxidation and *N*-terminal acetylation were searched as variable modifications and carbamidomethyl of cysteine as fixed modification. Parent peptide masses and fragment masses were searched with maximal mass deviation of 10 ppm. A first level of false discovery rate (FDR) filtration was done on the peptide-spectrum match level, and this was followed by a second level of FDR control on the protein level. Both filtrations were performed at a 1% FDR. These filtrations were done using a standard target-decoy database approach. For label-free relative quantification of the samples, the "match between runs" option of Proline was enabled to allow cross-assignment of MS features detected in the different runs. The minimal ratio count was set to 1 for calculation of abundances, which were used for relative quantification of proteins between the 3 groups of samples (CT, HD and LC). Missing data were implemented using the Imp4p-package (CRAN) working in Prostar.

Statistical analysis

Statistical analysis was performed with XLSTAT v2018.1 software (Addinsoft®). The tests were two sided, with a Type I error set at α = 0.05. Variables were presented as mean ± standard deviation or median [interquartile range] according to statistical distribution (assumption of normality assessed by the Shapiro–Wilk test). For demographic data and qRT-PCR results, a one-way analysis of variance (ANOVA) was used to compare values within the three groups, followed by post hoc Tukey test for pairwise comparison. For MS results analysis, a two-way ANOVA (group and replicate) was used to compare values in the three groups followed by Benjamini–Hochberg (BH) correction. Principal component analysis (PCA) was implemented on differentially expressed proteins. To focus on the proteins whose expression best characterized atrophying muscles independently of the disease (HD or LC vs. CT), we performed orthogonal partial least square discriminant analysis (O-PLS-DA). Proteins were classified according to their variable importance

in projection (VIP). A VIP > 1 was considered for selecting the proteins.[32] Proteins whose VIP was above 1 and significantly increased or decreased in both LC and HD patients were then evaluated using unsupervised hierarchical clustering (*k*-means classification and hierarchical ascending classification centred on Euclidean distances).

Bioinformatic analysis of protein expression data

Bioinformatic analysis was performed using Cytoscape software v3.6.0.[33] Proteins whose VIP was above 1 and concomitantly increased or decreased in LC and HD patients when compared with CT patient were considered as common markers of muscle atrophy process. Identification of the functions of these proteins was implemented with ClueGO v2.5.0.[34] A network of Gene Ontology biological process was created allowing to group the redundant term in functional cluster. Enrichment analysis was then performed for each cluster. GO levels 5 to 15 were considered. The kappa-statistics score threshold to create edge between nodes was set to 0.56. A two-sided (enrichment/depletion) hypergeometric test followed by BH correction was used to perform enrichment analysis. Group fusion option was used to diminish the redundancy of the terms shared by similar associated proteins, which allows to maintain the most representative parent or child GO term. Then, a gene network analysis was implemented with CluePedia v1.5.0[35] using the String protein interaction database (January 2018) in order to identify potential activated or repressed pathways. In order to validate our results, a protein co-expression network was created based on the Spearman rank correlation at a threshold of 0.6. Then, clustering was made using ClusterOne.[36] Finally, for each cluster, identification of the most enriched functions/pathways was performed using GeneMANIA v3.4.1 and default settings.[37]

Results

Patients' demographic

Demographic characteristics of the 21 patients included in this study (*n* = 7 per group) are shown in *Table 1*. The three groups differed neither in age nor in sex ratio with a majority of men included. The body mass index of patients in the LC and HD groups was not significantly different compared with patients in the CT group, and it remained within the normal range. Systemic inflammation assessed by the CRP measurement was normal in the CT group (3.0 mg/L) for 70 years old patients and was significantly higher (more than three-fold to four-fold) in the LC and HD patients. Glomerular filtration rate estimated by the Chronic Kidney Disease Epidemiology Collaboration equation was similar in the CT and LC groups and within the normal range considering the age of the patients.

Table 1 Demographic characteristics of the patients

	Control patients ($n = 7$)	Lung cancer patients ($n = 7$)	Haemodialysis patients ($n = 7$)	P
Age (years)	71 [60–79]	69 [62–75]	69 [66–77]	>0.9
M:F	6:1	6:1	6:1	>0.9
Weight (kg)	76 [73–78][a]	66 [62–72][ab]	64 [59–66][b]	0.05
Height (cm)	170 [174–182][a]	173 [169–176][ab]	165 [160–170][b]	0.03
BMI	24.8 [23.5–25.1]	21.3 [20.2–24.1]	23.4 [22.4–24.4]	0.15
CRP (mg/L)	3.0 [3.0–7.4][a]	9.7 [4.1–37.3][b]	12.8 [4.4–22.5][b]	0.03
Creatinine (μmol/L)	66 [59–81][a]	82 [64–90][a]	535 [494–752][b]	<0.001
GFR (mL/min/1.73 m^2)	88 [85–95]	84 [74–94]	NA	>0.9

BMI, body mass index; CRP, C-reactive protein; GFR, glomerular filtration rate; M:F, sex ratio male-to-female; P-value obtained with one-analysis of variance.
Values are median and interquartile range.
Values with different letters are significantly different using Tukey multiple comparison post hoc test.

The ubiquitin proteasome system and autophagy proteolytic system are activated in the muscle of lung cancer and haemodialysis patients

Studies conducted on cells or animal models have identified several genes whose expression is modified during muscle atrophy. These genes, called atrogenes, are markers of muscle wasting. Notably, they belong to cellular proteolytic systems such as the UPS and autophagy. In order to address the activation of atrophy in LC and HD patients, qRT-PCR was performed to quantify in muscles biopsies the expression of several genes belonging to several proteolytic systems. Atrogenes include several E3 ligases of the UPS, which are often good markers of atrophy. We thus addressed different E3 ligases that have been described for their implication in muscle homeostasis. MuRF1, MAFbx, Hdm2, and Fbxo30/MUSA1 E3 ligases were up-regulated at the mRNA levels in the muscle of LC and HD patients when compared with the CT group (*Figure 1(A)*). In contrast, Nedd4, E4b, and Trim32 transcripts were only up-regulated in patients from the HD group, while no variation was observed for Ozz (*Figure 1(A)*). E3 ligases work in couple with E2 Ub-conjugating enzymes to ensure the ubiquitination of their substrate. We therefore quantified the expression of several E2s already described for being up-regulated in several catabolic situations in rodents (*Figure 1(B)*). However, only UBE2E1 and UBE2V2 transcripts were increased in LC patients and UBE2A and UBE2J1 in HD patients. We then addressed 26S proteasome subunits, but surprisingly, no significant variation was found for the 20S complex subunits (*Figure 1(C)*). For the 19S regulatory complex (19S RC), only an increase in PSMD13 mRNA levels was found in both LC and HD patients, while PSMD2 and PSMD4 were up-regulated only in HD patients (*Figure 1(D)*). We selected CTPL and p62/SQSTM1 as markers of the autophagy proteolytic system. Increased mRNA levels of both CTPL and p62/SQSTM1 were found in both LC and HD patients (*Figure 1(E)*), suggesting that autophagy was activated. Muscle atrophy may also be accompanied by apoptosis of muscle cells. Indeed, we found increased levels of the pro-apoptotic

Casp3, Casp9, and Bax transcripts and a decrease of the anti-apoptotic Bcl2, but the modifications were restricted to HD patients (*Figure 1(F)*). Altogether, our data suggest an up-regulation of the UPS and the autophagy proteolytic systems, the most sensitive markers of the UPS being E3 ligases, that is, enzymes that select the proteins to be degraded.

A specific proteome identifies atrophying muscle independently of the aetiology of the disease

As we found an increased transcription of atrophying genes in muscles from LC and HD patients, we then addressed potential changes in the muscle proteome. MS analysis of the cytoplasmic fraction identified 1779 proteins (Supporting Information, *Table S2*), of which 919 were differently expressed in at least one group ($P < 0.05$ ANOVA for group factor after BH correction). Out of them, 257 proteins were increased or decreased in both LC and HD patients when compared with CT patients (*Figure 2(A)*). Moreover, LC/CT and HD/CT expression ratios of these proteins were well correlated, indicating that their variation levels were highly similar independently of the disease (*Figure 2(B)*).

Principal component analysis was performed on proteins differently expressed between the three groups (*Figure 3(A)*). PCA allows reducing the number of correlated variables to a limited number of independent variables (principal components) that better explain the observed variance. PCA grouped the proteins into three distinct sectors of the space generated by the two principal components, which nicely fitted respectively to the CT, LC, and HD groups (*Figure 3(A)*). This indicates that each patient's group exhibited a specific proteome and that a distinct signature can be drawn for CT, LC, and HD patients.

We then decided to focus on proteins that best characterized atrophying muscles independently of the causal pathology, and we performed an O-PLS-DA (*Figure 3(B)*). The horizontal component of the O-PLS-DA score scatter plot captures variation between the groups (LC or HD vs. CT), and the

Figure 1 Quantitative real-time PCR of genes from ubiquitin proteasome system and autophagy proteolytic system. mRNA levels of several components from ubiquitin proteasome system and autophagy proteolytic system are increased in muscle of LC and HD patients. *P*-value obtained with one-way analysis of variance. Values with different letters are significantly different using Tukey multiple comparison post hoc test. CT, healthy; HD, haemodialysis; LC, lung cancer.
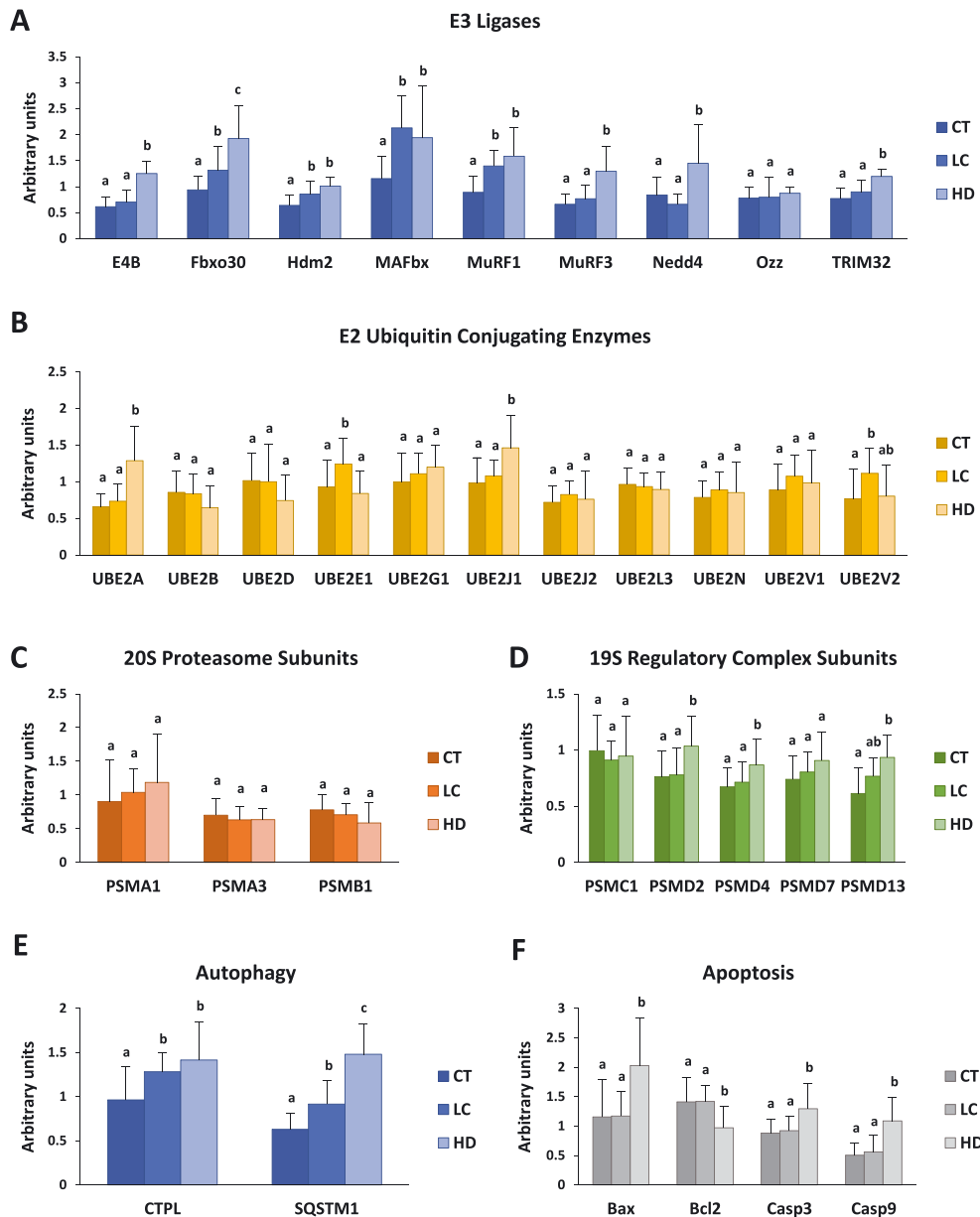
vertical component captures variation within the groups. The model obtained exhibited an R^2 (measure of model fit to the original data) of 0.993 and a Q^2 (internal measure of consistency between the original and cross-validation predicted data) of 0.983. The contribution of proteins to the model was evaluated by the calculation of the VIP. We found 321 proteins exhibiting a VIP > 1, which was considered the threshold for selecting the proteins[32] (*Figure 3(C)*). By crossing these data (321 proteins with a VIP > 1)

with those of the differential expression analysis (257 proteins that both increased or decreased in the LC and HD groups), we finally selected 238 proteins (Supporting Information, *Table S3*). Using an unsupervised hierarchical cluster analysis, we then addressed the capacity of these proteins for discriminating patients according to their original groups (*Figure 3(D)*). We found that a majority of proteins were potent indicators of catabolic conditions independently of the disease.

Figure 2 Shotgun proteomic analysis of muscle soluble proteome. (A) Volcano plots show differentially expressed proteins based on fold change vs. P-value obtained with analysis of variance after Benjamini–Hochberg correction. Proteins represented with red point are significantly ($P < 0.05$) increased or decreased in the muscles from both LC and HD patients. (B) Fold change in protein expression in LC vs. HD patients relative to CT patients. Change in expression of commonly variant proteins was similar in LC and HD. CT, healthy; HD, haemodialysis; LC, lung cancer.
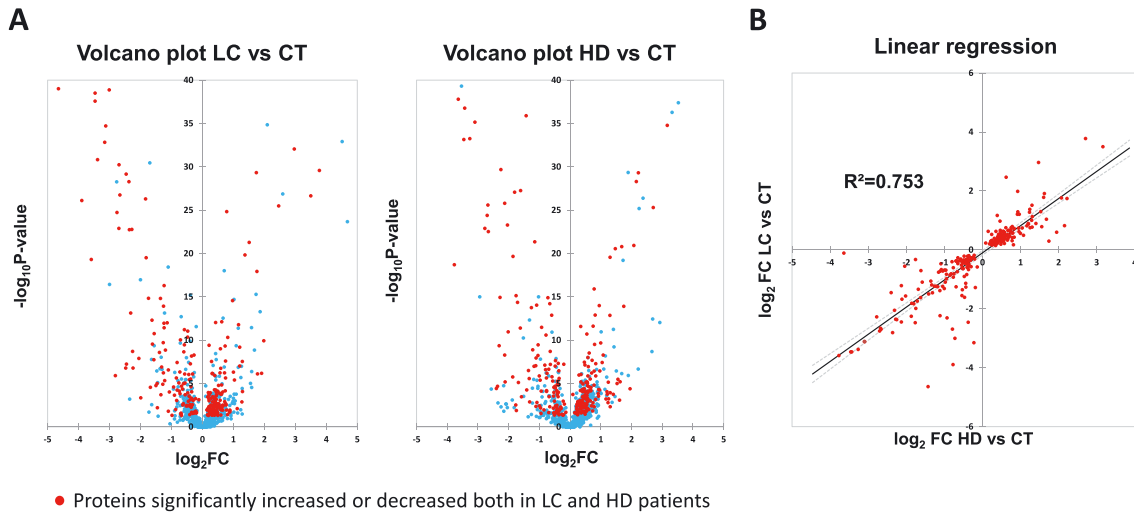

Figure 3 Multidimensional analysis of differentially expressed proteins in LC and HD groups. Each point represents one of the three patient replicates. (A) Principal components analysis reveals three different muscle soluble proteomes corresponding to the three different patients groups. (B) Based on differentially expressed proteins, O-PLS-DA creates a model allowing differentiating muscle of LC and HD patients from muscle of CT patients. (C) 321 proteins with VIP > 1 contribute significantly to the model. (D) For these 321 proteins, unsupervised hierarchical clustering identifies two different patterns of expression: proteins increased and proteins decreased in both LC and HD patients relative to CT patients. CT, healthy; HD, haemodialysis; LC, lung cancer; O-PLS-DA, orthogonal partial least square discriminant analysis; PCA, principal component analysis; VIP, variable importance in projection.
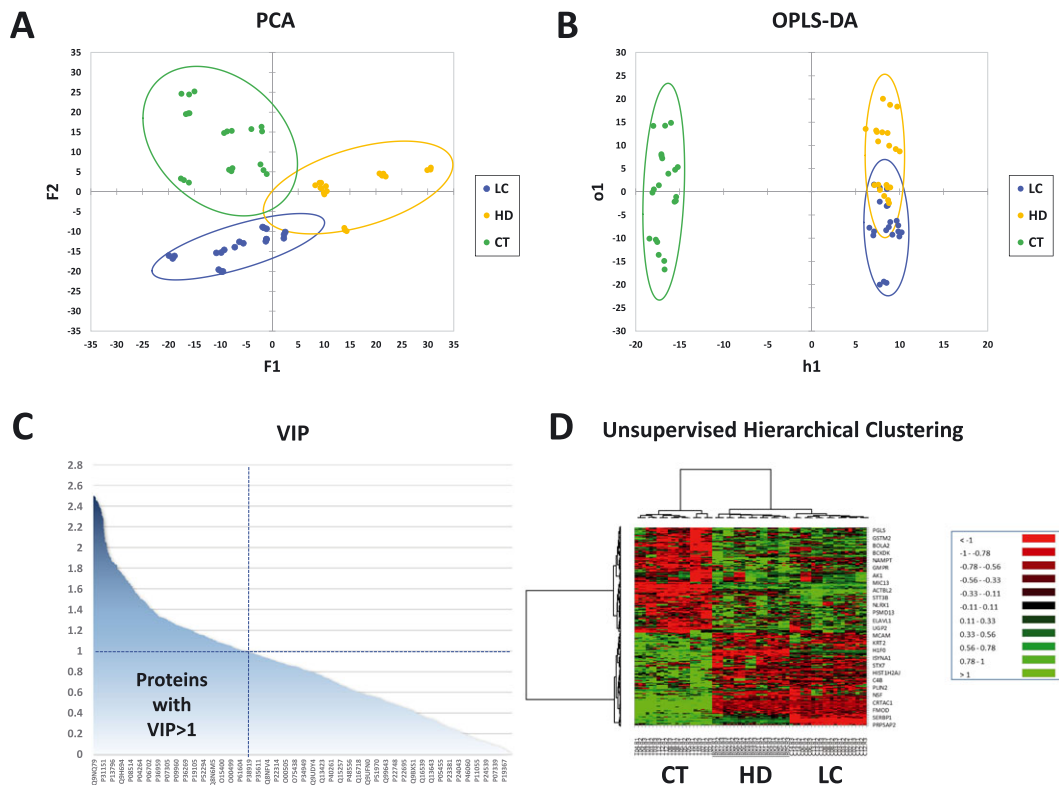
Biological processes modified upon muscle atrophy

We carried out a functional analysis of the 238 proteins that best witnessed muscle atrophy using the ClueGO plug-in. This revealed that these proteins can be grouped in functional modules related to biological processes significantly enriched when compared with the healthy human proteome (*Figure 4(A)* and *4(B)*). Overall, it included several metabolic pathways (proteostasis, glucose catabolic process, fatty acid, and energy metabolism), inflammation, defence against free oxygen radicals, structural proteins (cytoskeleton organization and extracellular matrix protein), and proteins involved in muscle contractile function (*Table* 2). Regarding proteolysis, we found an increase of several proteins related to the UPS and the autophagy proteolytic systems (*Figure 4(C)*). To confirm these results, we used a different approach. A co-expression network was created from the 1759 proteins identified in MS. It was a scale-free network with a node degree distribution following a power law ($R^2 = 0.93$), confirming its biological relevance (*Figure 5*). Using the ClusterOne algorithm, proteins have been grouped into 50 clusters of co-expression. Eight cluster displayed enriched functions (cellular respiration, inflammatory response, leucocyte migration, translation factor activity, muscle contraction, extracellular matrix, glucose metabolic process, and proteasome pathway) (*Table* 3).

The Wnt-β-catenin and ATF4 signalling pathways are up-regulated in both haemodialysis and lung cancer patients

In order to identify signalling pathways potentially involved, a protein interaction network analysis was performed using CluePedia software. Ten proteins characterizing pathological muscles belonged to the Wnt-β-catenin pathway, which suggested an activation of this signalling pathway (*Figure 6(A)*). Similarly, ERp44 an endoplasmic reticulum (ER) stress marker was significantly increased in atrophying muscles, and we thus checked whether the ATF4 pathway was activated in the patients' muscles. We found a significant increase of ATF4, CHOP, and 4EBP1 transcripts in both LC and HD patients when compared with CT patients (*Figure 6(B)*).

Discussion

In this study, we focused on skeletal muscle proteolysis and proteome modifications induced by two diseases (LC and HD) with a different aetiology and known to induce muscle atrophy in humans. We first found that the UPS and the autophagy proteolytic systems were concomitantly activated in both LC and HD patients and that some E3 ligases are

Figure 4 Functional enrichment analysis. (A) Proteins whose expression characterize pathological muscle from lung cancer and haemodialysis patients are involved in proteolysis, protein folding, amino acid metabolism, glucose catabolic process, fatty acid metabolic process, oxidative phosphorylation, regulation of inflammatory response, leucocyte migration, cellular oxidant detoxification, regulation of cytoskeleton organization, extracellular matrix, and striated muscle contraction. (B) Most proteins belong to the inflammatory response and proteostasis processes. (C) Proteins involved in proteolysis and modified in both lung cancer and haemodialysis patients belong to the ubiquitin proteasome system and autophagy proteolytic system.
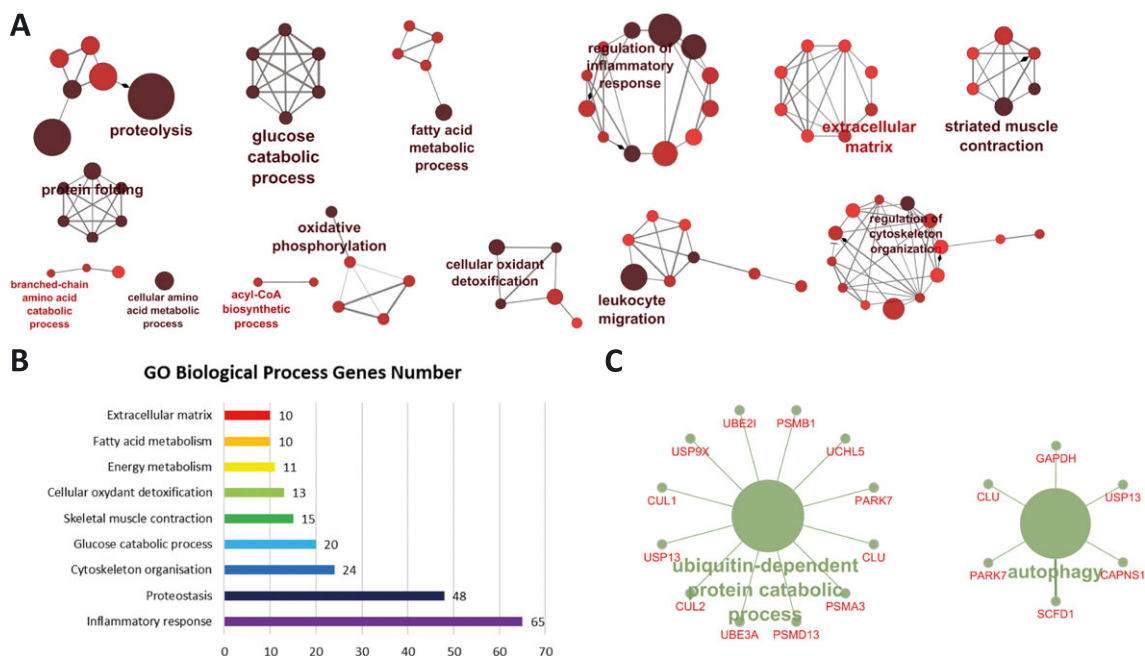
Table 2 Enriched biological process in LC and HD patients

	Increased expression	Decreased expression	Enrichment P-value
Proteostasis			
Proteolysis	CAPNS1, CTTNB, CUL1, CUL2, I, PSMA3, PSMB1, PSMD13, GAPDH,, NPEPPS, QDPR, SCFD1, PGEP1, SERPINB1, SERPINB6, UBE2I, USP9X	APCS, ASPN, AZU1, BGN, CASP14, CLU, PARK7, PIP, SERPINB3, UBE3A, USP13, UCHL5	2,6E−7
Protein folding	BOLA2, GNB1, CLU, APCS, HSPA6, B2M, ERP44, PPIH, TXNDC5, HSPA1B PARK7, STT3B	AHSA1, HSPE1	1.7E−3
Cellular amino acid metabolic process	AARS, AIMP1, BCKDK	ADI1, DBT, DDAH2,	5E−3
Glucose catabolic process	AKR1B1, ENO2, ENO3, GAPDH, GPD1, PFKFB1, PFKFB2, PGAM1, PGAM2, PGK1, PGLS, PGM1, PHKA1, PHKG1, PGPEP1, PKM, PTBP1, LDHD, UGP2,	SORD	2.5E−7
Fatty acid metabolism	ACAD9, AKR1C2, ECHDC2, FTO, HSD17B12, GPD, PLIN2, ZADH2	ACAA1, CDS2	1,4E−4
Energy metabolism			
Acetyl Co A biosynthetic process	ACSS1, LDHD	MPC1	5.2E−4
Oxidative phosphorylation	NDUFA1, MRP44, MIC13	ATP5D, DMAC1, SARS2, USP13, VGF	5E−3
Inflammatory response			
Regulation of defence response	ABCE1, AIMP1, ARPC1A, B2M, CUL1, F13A1, FGA, FGB, FGG, GAPDH, GRB2, IGHD, HSP1A, LTA4H, NLRX1, PSMA3, PSMB1, PSMD13, PTGIS, SAMHD1, SERPINB1, STAT3, SCNA	APCS, AZU1, BPI C4B, C5, MPO, PRTN3, CD47, CFHR2, KRT1, LCN2, LGAL3, NOS2, PARK7, PCBP2, PROS1, SAA, S100A7, S100A8, S100A9	3.3E−7
Leucocyte migration	AIMP1, BOLA2, CD47, GRB2, IGKV4–1, PRTN3, RHOA, STAT3	ADD2, AZU1, C5, CLU, GYPA, IGLV1–47, LCP1, LGALS3, MPP1, PROS1, SAA1, S100A7, S100A8, S100A9	1,8E−5
Extracellular matrix	FBLN5, GMPPB, PEPD, SERPB1	APCS, ASPN, BGL, CILP, FMOD, PIP	3.4E−02
Skeletal muscle contraction	CFL2, CSRP3, KELCCH, KLHL41, MYL4, MYH15, MYPN, ANXA6, ATP1A2, GPD1-L, NIPSNAP2	MYH6, NRAP, PLN, SLC20A2	8,5E−4
Cytoskeleton organization	ACTBL2, ARHGDIA, ARPC1A, CFL2, CTNNB1, GDI1, NUBP2, PFN2, PRUNE1, RHOA, SNCA	ADD2, DMTN, FLNA, JUP, KRT1, KRT2, LCP1, MYOC, PALM, S100A8, S100A9, TUBA1A, TUBB1	1.3E−4
Cellular oxidant detoxification	AKR1B1, CCS, FAM213A, FBLN5, GSTM2, GSTT1, MPO, NUP93, NQO1, PARK7, S100A9, TXNRD, HAGH		9.9E−6

Enriched biological process have been identified from the 321 proteins whose expression was significantly increased or decreased in both lung cancer (LC) and haemodialysis (HD) patients, using ClueGO® plug-in in Cytoscape®.

potent markers of human muscle atrophy. We then found a panel of 238 proteins belonging to nine main cellular functions that characterized atrophying muscles independently of the disease. Finally, we found that the Wnt-β-catenin and ATF4 signalling pathways were activated in both HD and LC muscles. This study was conducted with a limited number of patients, and the differential proteins (and mRNAs) will have to be confirmed using larger cohorts of patients, by focusing on the most variable markers.

In various models of rodent muscle atrophy, several genes are systematically overexpressed at the transcriptional level, and these atrophy-related genes (atrogenes) include members of the main proteolytic systems (UPS and autophagy).[6,38] Regarding the UPS, atrogenes include Ub, 20S proteasome subunits, 19S regulatory complex subunits, and ubiquitinating enzymes (E2s and E3s). Indeed, both substrate targeting (ubiquitination) and degradation (26S proteasome) steps are up-regulated in various catabolic situations (fasting, diabetes mellitus, renal failure, tumour bearing, and hindlimb suspension).[17,39,40] Surprisingly, in this study, proteasome subunits (belonging either to the 20S proteasome core or to the 19S regulatory complex) appeared to be poor predictors of the atrophying process in humans. Indeed, none of the 20S and 19S RC subunits tested were up-regulated in both LC and HD patients at the mRNA levels, and only three of them were increased at the protein levels (*Figure 1(C)* and *1(D)*, *Table 2*, and Supporting Information, *Table S1*). E2 enzymes appeared also to be poor predictors of muscle atrophy in LC and HD patients (*Figure 1(B)* and Supporting Information, *Table S1*) in contrast with animal models in which UBE2B was considered as a bona fide atrogene and other E2s were often upregulated during catabolic situations (see Polge *et al.*[41] for compiled data).

Several E3 ligases were up-regulated in both LC and HD patients and more particularly MuRF1 and MAFbx, two muscle-specific E3 ligases considered as the best markers of muscle

Figure 5 Proteins co-expression network analysis. Spearman rank correlation for expression of all possible protein pair is calculated. In graph, proteins are represented with nodes, and an edge is created between two nodes if the Spearman rank correlation for the expression of the two proteins among all patients is above 0.6. Node degree distribution followed a power law. The ClusterOne algorithm led to the identification of 50 clusters of co-expressed proteins.
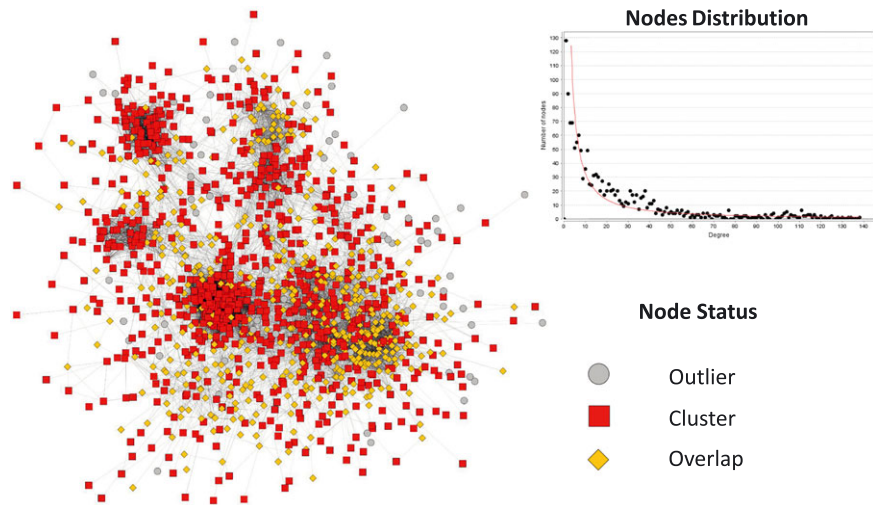

Table 3 Functions of clusters of expression

Cluster	Enriched function	Q-value	Proteins involved
1	Cellular respiration	1.0E−161	ACO2, ALDH5A1, ATP5A1, ATP5B, ATP5C1, ATP5D, ATP5F1, ATP5H, ATP5I, ATP5J2, ATP5L, ATP5O, COX4I1, COX5A, COX5B, COX6B1, COX6C, CS, CYC1, CYCS, DLD, DLST, ETFA, ETFB, ETFDH, FH, IDH2, IDH3A, IDH3G, MDH2, MT-ATP6, MT-CO2, NDUFA10, NDUFA11, NDUFA12, NDUFA13, NDUFA2, NDUFA4, NDUFA5, NDUFA6, NDUFA8, NDUFA9, NDUFAB1, NDUFB1, NDUFB10, NDUFB11, NDUFB3, NDUFB4, NDUFB5, NDUFB6, NDUFB7, NDUFB8, NDUFB9, NDUFC2, NDUFS1, NDUFS2, NDUFS3, NDUFS4, NDUFS6, NDUFS7, NDUFS8, NDUFV1, NDUFV2, NNT, OGDH, PDHA1, PDHB, SDHA, SDHB, SLC25A12, SLC25A13, SUCLA2, SUCLG1, UQCRB, UQCRC1, UQCRC2, UQCRFS1, UQCRH
2	Inflammatory response	7.9E−18	A2M, AGT, AHSG, APOA1, APOD, APOE, C3, C4A, C9, CFB, CFH, ITIH4, KNG1, ORM1, SERPINA3, SERPING1, VTN
3	Leucocyte migration	2.3E−06	AZU1, CD47, ITGB3, MPP1, PROS1, S100A7, S100A8, SAA1
4	Translation factor activity	4.5E−10	EEF1A2, EIF2S1, EIF3E, EIF3I, EIF4A2, EIF4G1
5	Muscle contraction	1.1E−58	TPM1, TMOD4, TNNT3, MYL1, TNNI2, TPM2, MYH7, MYH2, TPM3, ACTN3, TMOD1, MYL3, ASPH, MYL6B, TNNI1, MYL5, MYH3, ACTN2, TNNT1, TNNC1, ACTA1, MYBPC2, MYL2, MYH4
6	Extracellular matrix	4.4E−5	COL15A1, CILP, SNCA, FMOD
7	Glucose metabolic process	2.6E−36	PGK1, PGAM2, ALDOA, ENO2, PGM1, FBP2, GAPDH, ENO3, GPI, ALDOC, TPI1
8	Proteasome complex	1.1E−71	PSMA5, PSMA3, PSMD6, PSMD4, VCP, PSMA1, PSMB7, PSMB1, PSMA7, PSMB2

Eight clusters of expression identified using ClusterOne® display enriched function in GeneMania®.

atrophy in rodents.[6,42] Even though human studies are relatively scarce compared with rodent, several investigations also observed an up-regulation of MuRF1 and MAFbx following immobilization, spinal cord injury, or chronic obstructive pulmonary disease.[6] The sustained up-regulation of these E3 ligases over years (HD patients) suggests that both an increased degradation of the contractile apparatus (i.e. MuRF1 targets like α-actin, myosin heavy chains, and telethonin) and a repression of protein synthesis and anabolic factors (i.e. MAFbx targets like eIF3f and MyoD) are necessary for maintaining long-term muscle atrophy.[7–9,41,43] In our study, we also found that two other E3 ligases were up-regulated at

the mRNA level, that is, human double minute (Hdm2) and F-box protein 30/muscle Ub ligase of the SCF complex in atrophy-1 (Fbxo30/MUSA1). Hdm2 is a ubiquitous E3 ligase mostly known for its role in p53 ubiquitination during cancer development, but it is also up-regulated in muscles from hindlimb suspended rats, a model of hypokinesia.[17] Finally, Fbxo30/MUSA1 is a muscle-specific E3 ligase that was described as essential for the development of muscle atrophy in several rodent models with the exception of mild renal failure in rats, but Fbxo30/MUSA1 targets remain to be discovered.[10,42,44–46] The recruitment of E3 ligases in catabolic patients was further demonstrated at the proteome level.

Figure 6 Signalling pathways activated in lung cancer (LC) and haemodialysis (HD) patients. (A) Analysis based on String protein interaction database predicts that the Wnt pathway signalling is activated in LC and HD patients. (B) Increased mRNA levels of ATF4, CHOP, and 4EBP1 revealed activation of the ATF4 pathway in both LC and HD patients.
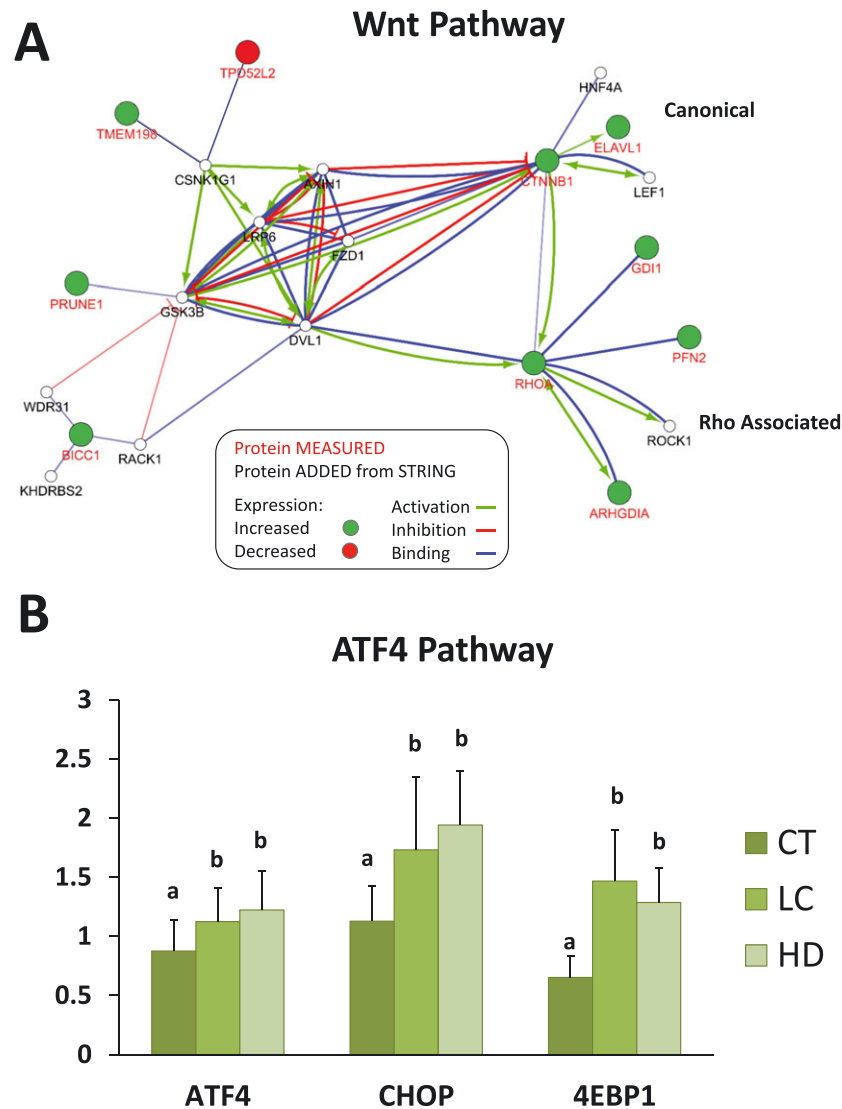
Indeed, we found that the Cul1 and Cul2 were up-regulated in both LC and HD patients (*Table* 2 and Supporting Information, *Table S3*). Cul1 and Cul2 are scaffold proteins included in several multi-subunits Cullin-Ring E3 ligases, which means that numerous E3 ligases belonging to this family may be up-regulated in LC and HD patients. Interestingly, Cul1 is the Cullin integrated to the multi-subunits MAFbx E3 ligase, which corroborates the data obtained at the mRNA level. Altogether, we found that several components of the UPS were up-regulated in both LC and HD patients (*Figure 1*, *Table* 2, and Supporting Information, *Table S3*) but this was restricted to E3 ligases, which is in striking contrast with rodent models. The main difference between animal models and human pathologies is the timing, which is generally in days for animal models while it is in months or years for humans. Indeed, even though we recruited LC patients soon after cancer discovery, the atrophying process was probably already activated for weeks. However, body mass index was within the normal range, which suggests that LC and HD patients were not severely cachectic. We hypothesize that the 26S proteasome and the E2 enzymes do not need to be maintained up-regulated once the pathology is established, the enzyme activity being sufficient for maintaining the skeletal muscle in a catabolic state. In contrast, some E3 ligases (MuRF1, MAFbx, Hdm2, and Fbxo30/MUSA1) are involved in the atrophying programme in both very early (3–7 days, rodents) and late (>1 year, humans) stages of muscle atrophy.

Autophagy is known for playing a crucial role in atrophying muscles from rodents,[10,47,48] and we found that p62/SQSTM1 was up-regulated in LC and HD patients. p62 is a cargo recognition protein implicated in the selective addressing of proteins (or protein aggregates) or organelles to the autophagy machinery. Increased p62 transcription levels are thus directly linked to an increased autophagy flux. We also found that cathepsin L (CTPL) and myosin heavy chain 15 (MYH15) were also up-regulated in both LC and HD patients. CTPL is a lysosomal protease (the catalytic organelle of autophagy) and is also known to be an atrogene in rodent muscles.[17,40] MYH15 is a heavy chain of myosin involved in the transport of lysosomal vesicles. Our data are in accordance with previous studies demonstrating that LC3B (a protein crucial for autophagosome formation) and CTPL were up-regulated in muscles from cancer cachexia patients.[49] Similarly, autophagy was activated in nephrectomized mice, causing mitochondria dysfunction without affecting the contractile apparatus.[50] Altogether, key proteins of autophagy were up-regulated in both LC and HD patients, which represent potent and persistent markers of muscle atrophy.

Another main goal of our study was to find a shared atrophying pattern in patients developing diseases with a completely different aetiology and at different stages. Our hypothesis was that similar protein modifications in LC and HD patients are more likely due to the atrophying process rather than the pathology itself. Interestingly, we found 238 proteins that were either down-regulated or up-regulated in both LC and HD patients. Interestingly, numerous proteins of unknown function (at least in skeletal muscle) were among the ones undergoing the sharpest modifications. For example, several proteins positively correlating with cellular proliferation were down-regulated, such as dermcidin (−76 to −80%, $P < 1.0E-07$). Future studies will have to investigate the role of these proteins in the development of muscle atrophy, but one hypothesis is that a sustained repression of cell proliferation may be an adaptive mechanism of muscle atrophy.

Besides proteins of unknown functions, our data highlighted an activation of ER stress in both LC and HD patients. We found that several chaperones were up-regulated in the skeletal muscle of these patients, notably ERp44 a marker of ER stress (+234 to +368%, $P < 1.0E-29$). ERp44 is a pH-regulated chaperone of the secretory pathway, which controls oxidative-related protein misfolding in the ER.[51] These results are in accordance with studies showing that ER stress is activated in several catabolic situations (denervation, starvation, high-fat diet, cancer cachexia, and ageing).[52] The ER stress response can be activated by several stress factors (nutrient deprivation, reactive oxygen species, etc.) and more recently in mice injected with indoxyl sulfate, a uraemic toxin.[53] However, it is the first time that an ER stress is detected in HD patients. The ER stress response involves in particular the PERK/ATF4/CHOP signalling pathway that decreases overall protein translation, triggers the specific expression of chaperones, activates the UPS and autophagy proteolytic systems, and may ultimately lead to apoptosis.[54] Accordingly, we found an up-regulation of CHOP, ATF4, and 4EBP1 (a downstream key protein of this pathway) in the muscles from both LC and HD patients (*Figure 6(B)*).

Another striking effect of both cancer and renal failure was the increased expression of several glycolytic enzymes and the down-regulation of several proteins involved in mitochondrial respiration in the muscle from LC and HD patients (*Tables* 2 and 3). This is in agreement with the slow oxidative to fast glycolytic transformation process observed during muscle atrophy[55] and the increased expression of several glycolytic enzymes observed in atrophying muscles from hindlimb suspended,[56] denervated,[57] or immobilized[58] animals. Mitochondrial dysfunction has also been found in different rodent models of cachexia[50,59] and is a regulator of myofiber protein turnover and apoptosis.[60] The proposed model is that mitochondrial dysfunction may precede the installation of muscular atrophy.[61] Increased reactive oxygen species[62] and inflammation[63] have also been proposed to explain the metabolic changes associated with muscle atrophy. Future studies will have to clarify the role of the modifications in the occurrence of muscle wasting.

Muscle atrophy is accompanied by modifications of proteins involved in contraction and in the architecture of muscle tissue, including cytoskeleton,[64] increased muscle fibrosis,[65] and adipogenic infiltration.[66] In mice subjected to hindlimb suspension, the expression of several cytoskeleton proteins was modified in the atrophying muscles.[64] A remodelling of the cytoskeleton appears essential for allowing the degradation of filamentous proteins and for preserving the functional integrity of myofibrils during muscle atrophy.[67] Similarly, several proteins involved in muscle architecture and muscle contraction were either down-regulated or up-regulated in both LC and HD patients (*Table* 2). Indeed, a group of proteins whose expression levels were modified in the muscle of LC and HD patients belong to the cytoskeleton organization including intermediate filaments. We found an up-regulation of ARPC1A (component of the ARP2/3 complex), cofilin 2 (CFL2), and profilin 2 (PFN2) (regulators of actin polymerization/depolymerization) and a down-regulation of filamin A (FLNA) (a cellular actin-network stabilizer) and junction plakoglobin (JUP) (a mechanical stress transduction protein). We have also noted increased levels of myopalladin (MYPN), a protein that participates to thin filament assembly by linking nebulin and α-actinin.[68] Its translocation into the cytosol may witness the destabilization of the sarcomeric structure and the subsequent degradation of sarcomeric proteins by the UPS. Furthermore, profound modifications of extracellular matrix components were observed between control and diseased patients (*Table* 2) like peptidase D (PEPD) (+15 to +40%, $P < 1.0E-02$), a protein involved in collagen synthesis, and the acireductone dioxygenase 1(ADI1),

an extracellular protease inhibitor (-39 to -61%, $P < 1.0E-04$), which further suggest a profibrotic process in skeletal muscles from LC and HD patients. Regarding muscle adiposity, we found an increase in fat tissue obesity gene expression ($+14$ to $+40\%$, $P < 1.0E-02$). Fat tissue obesity is a nucleic acid demethylase that controls the expression of genes involved in energy metabolism. Its overexpression has been shown to cause intracellular lipid accumulation in skeletal muscle cells[69] and increased white adipose tissue.[70] Interestingly, proteome analysis also revealed an activation of the Wnt/β-catenin pathway in both groups, which is known to have a dual function as it is involved either in muscle regeneration[71] or in fibrosis.[72] Inhibition of canonical Wnt signalling in aged skeletal muscle has the potential to reduce fibrosis development.[72] This suggests that targeting the canonical Wnt pathway may be a potential approach for preserving muscle integrity.

The discovery of >230 proteins differentially expressed in the HD and LC patients has several implications. First, it means that profound modifications of skeletal muscle metabolism occur and that they persist throughout the course of the pathology. Thus, the identified markers are potentially interesting not only for characterizing muscle atrophy but also for better understanding the atrophy process. The second point is that these markers were not equally modified; that is, some of them reached a five-fold to seven-fold increase while others were 'only' increased by 50%. This does not mean the higher the better. Future studies will have to identify the most reliable markers, that is, the ones systematically altered in most if not all patients and predictive of muscle mass loss when using larger cohorts. The third important implication is that these muscle markers will be hardly useful for direct clinical use (muscle biopsies). We are currently working on the detection of blood markers that could reflect the atrophying programme observed in skeletal muscle, this study being an obligatory and highly valuable step.

Conclusions

We observed an activation of the UPS and autophagy proteolytic systems and common proteomic modifications in atrophying skeletal muscles from LC and HD patients. Our data suggest that the degradation of the contractile apparatus and of the muscular cell structure (cytoskeleton) may be highly similar whatever the pathology, which means similar therapeutic strategies may be applied for preserving muscle

mass. Our work represents a proof of concept with a limited number of patients, and future work will have to confirm these data on a larger number of patients with similar or different pathologies. Another important issue will be to determine whether the muscle-atrophying programme may also induce common variations in blood (e.g. at the transcriptomic level), a more easy-to-handle compartment in patients. If so, this may end up with a valuable diagnostic tool for early detection of catabolic situations or for following disease remission.

Acknowledgements

Online supplementary material

Additional supporting information may be found online in the Supporting Information section at the end of the article.

Table S1. List of primers
Table S2. Shot Gun expression data of muscle soluble proteome
Table S3. Protein with VIP > 1 and increased or decreased both in LC and HD patients

Conflict of interest

The authors declare that they have no conflict of interest. The authors certify that they comply with the ethical guidelines for publishing in the *Journal of Cachexia, Sarcopenia and Muscle*: update 2017.[73]

References

1. von Haehling S, Anker MS, Anker SD. Prevalence and clinical impact of cachexia in chronic illness in Europe, USA, and Japan: facts and numbers update 2016. *J Cachexia Sarcopenia Muscle* 2016; **7**:507–509.

2. Kalantar-Zadeh K, Rhee C, Sim JJ, Stenvinkel P, Anker SD, Kovesdy CP. Why cachexia kills: examining the causality of

poor outcomes in wasting conditions. *J Cachexia Sarcopenia Muscle* 2013;**4**:89–94.

3. Argiles JM, Busquets S, Stemmler B, Lopez-Soriano FJ. Cancer cachexia: understanding the molecular basis. *Nat Rev Cancer* 2014;**14**:754–762.

4. Baracos VE, Martin L, Korc M, Guttridge DC, Fearon KCH. Cancer-associated cachexia. *Nat Rev Dis Primers* 2018;**4**:17105.

5. Wang XH, Mitch WE. Mechanisms of muscle wasting in chronic kidney disease. *Nat Rev Nephrol* 2014;**10**:504–516.

6. Bodine SC, Baehr LM. Skeletal muscle atrophy and the E3 ubiquitin ligases MuRF1 and MAFbx/atrogin-1. *Am J Physiol Endocrinol Metab* 2014;**307**:E469–E484.

7. Polge C, Heng AE, Jarzaguet M, Ventadour S, Claustre A, Combaret L, et al. Muscle actin is polyubiquitinylated *in vitro* and *in vivo* and targeted for breakdown by the E3 ligase MuRF1. *FASEB J* 2011;**25**:3790–3802.

8. Csibi A, Leibovitch MP, Cornille K, Tintignac LA, Leibovitch SA. MAFbx/Atrogin-1 controls the activity of the initiation factor eIF3-f in skeletal muscle atrophy by targeting multiple C-terminal lysines. *J Biol Chem* 2009;**284**:4413–4421.

9. Lagirand-Cantaloube J, Cornille K, Csibi A, Batonnet-Pichon S, Leibovitch MP, Leibovitch SA. Inhibition of atrogin-1/MAFbx mediated MyoD proteolysis prevents skeletal muscle atrophy *in vivo*. *PLoS One* 2009;**4**:e4973.

10. Milan G, Romanello V, Pescatore F, Armani A, Paik JH, Frasson L, et al. Regulation of autophagy and the ubiquitin-proteasome system by the FoxO transcriptional network during muscle atrophy. *Nat Commun* 2015;**6**:6670.

11. Tomko RJ Jr, Hochstrasser M. Molecular architecture and assembly of the eukaryotic proteasome. *Annu Rev Biochem* 2013;**82**:415–445.

12. Tisdale MJ. Cancer anorexia and cachexia. *Nutrition* 2001;**17**:438–442.

13. Bossola M, Tazza L, Giungi S, Luciani G. Anorexia in hemodialysis patients: an update. *Kidney Int* 2006;**70**:417–422.

14. Toledo M, Busquets S, Sirisi S, Serpe R, Orpi M, Coutinho J, et al. Cancer cachexia: physical activity and muscle force in tumour-bearing rats. *Oncol Rep* 2011;**25**:189–193.

15. Johansen KL, Chertow GM, Ng AV, Mulligan K, Carey S, Schoenfeld PY, et al. Physical activity levels in patients on hemodialysis and healthy sedentary controls. *Kidney Int* 2000;**57**:2564–2570.

16. Wing SS, Haas AL, Goldberg AL. Increase in ubiquitin-protein conjugates concomitant with the increase in proteolysis in rat skeletal muscle during starvation and atrophy denervation. *Biochem J* 1995;**307**:639–645.

17. Taillandier D, Aurousseau E, Meynial-Denis D, Bechet D, Ferrara M, Cottin P, et al. Coordinate activation of lysosomal, Ca 2+-activated and ATP-ubiquitin-dependent proteinases in the unweighted rat soleus muscle. *Biochem J* 1996;**316**:65–72.

18. Konishi M, Ishida J, von Haehling S, Anker SD, Springer J. Nutrition in cachexia: from bench to bedside. *J Cachexia Sarcopenia Muscle* 2016;**7**:107–109.

19. Patel HJ, Patel BM. TNF-alpha and cancer cachexia: molecular insights and clinical implications. *Life Sci* 2017;**170**:56–63.

20. Bonetto A, Aydogdu T, Jin X, Zhang Z, Zhan R, Puzis L, et al. JAK/STAT3 pathway inhibition blocks skeletal muscle wasting downstream of IL-6 and in experimental cancer cachexia. *Am J Physiol Endocrinol Metab* 2012;**303**:E410–E421.

21. Cai D, Frantz JD, Tawa NE Jr, Melendez PA, Oh BC, Lidov HG, et al. IKKbeta/NF-kappaB activation causes severe muscle wasting in mice. *Cell* 2004;**119**:285–298.

22. Wang X, Hu Z, Hu J, Du J, Mitch WE. Insulin resistance accelerates muscle protein degradation: activation of the ubiquitin-proteasome pathway by defects in muscle cell signaling. *Endocrinology* 2006;**147**:4160–4168.

23. Asp ML, Tian M, Wendel AA, Belury MA. Evidence for the contribution of insulin resistance to the development of cachexia in tumor-bearing mice. *Int J Cancer* 2010;**126**:756–763.

24. Costelli P, Muscaritoli M, Bonetto A, Penna F, Reffo P, Bossola M, et al. Muscle myostatin signalling is enhanced in experimental cancer cachexia. *Eur J Clin Invest* 2008;**38**:531–538.

25. Zhang L, Rajan V, Lin E, Hu Z, Han HQ, Zhou X, et al. Pharmacological inhibition of myostatin suppresses systemic inflammation and muscle atrophy in mice with chronic kidney disease. *FASEB J* 2011;**25**:1653–1663.

26. Zhang L, Pan J, Dong Y, Tweardy DJ, Dong Y, Garibotto G, et al. Stat3 activation links a C/EBPdelta to myostatin pathway to stimulate loss of muscle mass. *Cell Metab* 2013;**18**:368–379.

27. Gallagher IJ, Jacobi C, Tardif N, Rooyackers O, Fearon K. Omics/systems biology and cancer cachexia. *Semin Cell Dev Biol* 2016;**54**:92–103.

28. Workeneh BT, Rondon-Berrios H, Zhang L, Hu Z, Ayehu G, Ferrando A, et al. Development of a diagnostic method for detecting increased muscle protein degradation in patients with catabolic conditions. *J Am Soc Nephrol* 2006;**17**:3233–3239.

29. Bautmans I, Njemini R, De Backer J, De Waele E, Mets T. Surgery-induced inflammation in relation to age, muscle endurance, and self-perceived fatigue. *J Gerontol A Biol Sci Med Sci* 2010;**65**:266–273.

30. Mikura M, Yamaoka I, Doi M, Kawano Y, Nakayama M, Nakao R, et al. Glucose infusion suppresses surgery-induced muscle protein breakdown by inhibiting ubiquitin-proteasome pathway in rats. *Anesthesiology* 2009;**110**:81–88.

31. Chomczynski P, Sacchi N. Single-step method of RNA isolation by acid guanidinium thiocyanate-phenol-chloroform extraction. *Anal Biochem* 1987;**162**:156–159.

32. Lazraq A, Cléroux R, Gauchi JP. Selecting both latent and explanatory variables in the PLS1 regression model. *Chemom Intel Lab Syst* 2003;**66**:117–126.

33. Shannon P, Markiel A, Ozier O, Baliga NS, Wang JT, Ramage D, et al. Cytoscape: a software environment for integrated models of biomolecular interaction networks. *Genome Res* 2003;**13**:2498–2504.

34. Bindea G, Mlecnik B, Hackl H, Charoentong P, Tosolini M, Kirilovsky A, et al. ClueGO: a Cytoscape plug-in to decipher functionally grouped gene ontology and pathway annotation networks. *Bioinformatics* 2009;**25**:1091–1093.

35. Bindea G, Galon J, Mlecnik B. CluePedia Cytoscape plugin: pathway insights using integrated experimental and *in silico* data. *Bioinformatics* 2013;**29**:661–663.

36. Nepusz T, Yu H, Paccanaro A. Detecting overlapping protein complexes in protein–protein interaction networks. *Nat Methods* 2012;**9**:471–472.

37. Mostafavi S, Ray D, Warde-Farley D, Grouios C, Morris Q. GeneMANIA: a real-time multiple association network integration algorithm for predicting gene function. *Genome Biol* 2008;**9 Suppl 1**:S4.

38. Lecker SH, Jagoe RT, Gilbert A, Gomes M, Baracos V, Bailey J, et al. Multiple types of skeletal muscle atrophy involve a common program of changes in gene expression. *FASEB J* 2004;**18**:39–51.

39. Voisin L, Breuille D, Combaret L, Pouyet C, Taillandier D, Aurousseau E, et al. Muscle wasting in a rat model of long-lasting sepsis results from the activation of lysosomal, Ca2+-activated, and ubiquitin-proteasome proteolytic pathways. *J Clin Invest* 1996;**97**:1610–1617.

40. Temparis S, Asensi M, Taillandier D, Aurousseau E, Larbaud D, Obled A, et al. Increased ATP-ubiquitin-dependent proteolysis in skeletal muscles of tumor-bearing rats. *Cancer Res* 1994;**54**:5568–5573.

41. Polge C, Cabantous S, Deval C, Claustre A, Hauvette A, Bouchenot C, et al. A muscle-specific MuRF1-E2 network requires stabilization of MuRF1-E2 complexes by telethonin, a newly identified substrate. *J Cachexia Sarcopenia Muscle* 2018;**9**:129–145.

42. Aniort J, Polge C, Claustre A, Combaret L, Bechet D, Attaix D, et al. Upregulation of MuRF1 and MAFbx participates to muscle wasting upon gentamicin-induced acute kidney injury. *Int J Biochem Cell Biol* 2016;**79**:505–516.

43. Clarke BA, Drujan D, Willis MS, Murphy LO, Corpina RA, Burova E, et al. The E3 ligase MuRF1 degrades myosin heavy chain protein in dexamethasone-treated skeletal muscle. *Cell Metab* 2007;**6**:376–385.

44. Li F, Buck D, De Winter J, Kolb J, Meng H, Birch C, et al. Nebulin deficiency in adult muscle causes sarcomere defects and muscle-type-dependent changes in trophicity: novel insights in nemaline myopathy. *Hum Mol Genet* 2015;**24**:5219–5233.

45. Smith HK, Matthews KG, Oldham JM, Jeanplong F, Falconer SJ, Bass JJ, et al. Translational signalling, atrogenic and myogenic gene expression during unloading

and reloading of skeletal muscle in myostatin-deficient mice. *PLoS One* 2014;**9**:e94356.

46. Sato AY, Richardson D, Cregor M, Davis HM, Au ED, McAndrews K, et al. Glucocorticoids induce bone and muscle atrophy by tissue-specific mechanisms upstream of E3 ubiquitin ligases. *Endocrinology* 2017;**158**:664–677.

47. Masiero E, Agatea L, Mammucari C, Blaauw B, Loro E, Komatsu M, et al. Autophagy is required to maintain muscle mass. *Cell Metab* 2009;**10**:507–515.

48. Mammucari C, Schiaffino S, Sandri M. Downstream of Akt: FoxO3 and mTOR in the regulation of autophagy in skeletal muscle. *Autophagy* 2008;**4**:524–526.

49. Tardif N, Klaude M, Lundell L, Thorell A, Rooyackers O. Autophagic-lysosomal pathway is the main proteolytic system modified in the skeletal muscle of esophageal cancer patients. *Am J Clin Nutr* 2013;**98**:1485–1492.

50. Su Z, Klein JD, Du J, Franch HA, Zhang L, Hassounah F, et al. Chronic kidney disease induces autophagy leading to dysfunction of mitochondria in skeletal muscle. *Am J Physiol Renal Physiol* 2017;**312**: F1128–F1140.

51. Anelli T, Alessio M, Mezghrani A, Simmen T, Talamo F, Bachi A, et al. ERp44, a novel endoplasmic reticulum folding assistant of the thioredoxin family. *EMBO J* 2002;**21**:835–844.

52. Afroze D, Kumar A. ER stress in skeletal muscle remodeling and myopathies. *FEBS J* 2017.

53. Jheng JR, Chen YS, Ao UI, Chan DC, Huang JW, Hung KY, et al. The double-edged sword of endoplasmic reticulum stress in uremic sarcopenia through myogenesis perturbation. *J Cachexia Sarcopenia Muscle* 2018;**9**:570–584.

54. B'Chir W, Maurin AC, Carraro V, Averous J, Jousse C, Muranishi Y, et al. The eIF2alpha/ATF4 pathway is essential for stress-induced autophagy gene expression. *Nucleic Acids Res* 2013;**41**:7683–7699.

55. Bigard AX, Boehm E, Veksler V, Mateo P, Anflous K, Ventura-Clapier R. Muscle unloading induces slow to fast transitions in myofibrillar but not mitochondrial properties. Relevance to skeletal muscle abnormalities in heart failure. *J Mol Cell Cardiol* 1998;**30**:2391–2401.

56. Seo Y, Lee K, Park K, Bae K, Choi I. A proteomic assessment of muscle contractile alterations during unloading and reloading. *J Biochem* 2006;**139**:71–80.

57. Sun H, Liu J, Ding F, Wang X, Liu M, Gu X. Investigation of differentially expressed proteins in rat gastrocnemius muscle during denervation–reinnervation. *J Muscle Res Cell Motil* 2006;**27**:241–250.

58. Toigo M, Donohoe S, Sperrazzo G, Jarrold B, Wang F, Hinkle R, et al. ICAT-MS-MS time course analysis of atrophying mouse skeletal muscle cytosolic subproteome. *Mol Biosyst* 2005;**1**:229–241.

59. Argiles JM, Lopez-Soriano FJ, Busquets S. Muscle wasting in cancer: the role of mitochondria. *Curr Opin Clin Nutr Metab Care* 2015;**18**:221–225.

60. Carson JA, Hardee JP, VanderVeen BN. The emerging role of skeletal muscle oxidative metabolism as a biological target and cellular regulator of cancer-induced muscle wasting. *Semin Cell Dev Biol* 2016;**54**:53–67.

61. Brown JL, Rosa-Caldwell ME, Lee DE, Blackwell TA, Brown LA, Perry RA, et al. Mitochondrial degeneration precedes the development of muscle atrophy in progression of cancer cachexia in tumour-bearing mice. *J Cachexia Sarcopenia Muscle* 2017;**8**:926–938.

62. Tang H, Lee M, Sharpe O, Salamone L, Noonan EJ, Hoang CD, et al. Oxidative stress-responsive microRNA-320 regulates glycolysis in diverse biological systems. *FASEB J* 2012;**26**:4710–4721.

63. Remels AH, Gosker HR, Langen RC, Polkey M, Sliwinski P, Galdiz J, et al. Classical NF-kappaB activation impairs skeletal muscle oxidative phenotype by reducing IKK-alpha expression. *Biochim Biophys Acta* 1842;**2014**:175–185.

64. Wang F, Zhang P, Liu H, Fan M, Chen X. Proteomic analysis of mouse soleus muscles affected by hindlimb unloading and reloading. *Muscle Nerve* 2015;**52**:803–811.

65. Cisternas P, Henriquez JP, Brandan E, Inestrosa NC. Wnt signaling in skeletal muscle dynamics: myogenesis, neuromuscular synapse and fibrosis. *Mol Neurobiol* 2014;**49**:574–589.

66. Vettor R, Milan G, Franzin C, Sanna M, De Coppi P, Rizzuto R, et al. The origin of intermuscular adipose tissue and its pathophysiological implications. *Am J Physiol Endocrinol Metab* 2009;**297**:E987–E998.

67. Sanger JW, Wang J, Fan Y, White J, Mi-Mi L, Dube DK, et al. Assembly and maintenance of myofibrils in striated muscle. *Handb Exp Pharmacol* 2017;**235**:39–75.

68. Bang ML, Mudry RE, McElhinny AS, Trombitas K, Geach AJ, Yamasaki R, et al. Myopalladin, a novel 145-kilodalton sarcomeric protein with multiple roles in Z-disc and I-band protein assemblies. *J Cell Biol* 2001;**153**:413–427.

69. Wu W, Feng J, Jiang D, Zhou X, Jiang Q, Cai M, et al. AMPK regulates lipid accumulation in skeletal muscle cells through FTO-dependent demethylation of *N*(6)-methyladenosine. *Sci Rep* 2017;**7**:41606.

70. Merkestein M, Laber S, McMurray F, Andrew D, Sachse G, Sanderson J, et al. FTO influences adipogenesis by regulating mitotic clonal expansion. *Nat Commun* 2015;**6**:6792.

71. Rudolf A, Schirwis E, Giordani L, Parisi A, Lepper C, Taketo MM, et al. Beta-catenin activation in muscle progenitor cells regulates tissue repair. *Cell Rep* 2016;**15**:1277–1290.

72. Brack AS, Conboy MJ, Roy S, Lee M, Kuo CJ, Keller C, et al. Increased Wnt signaling during aging alters muscle stem cell fate and increases fibrosis. *Science* 2007;**317**:807–810.

73. von Haehling S, Morley JE, Coats AJS, Anker SD. Ethical guidelines for publishing in the *Journal of Cachexia, Sarcopenia and Muscle*: update 2017. *J Cachexia Sarcopenia Muscle* 2017;**8**:1081–1083.